# Aircraft Dutch Roll and State Variables Analysis Using Yaw Damper and Washout Filter

**Dr. Emad N. Abdulwahab***

Received on:29/9/2008
Accepted on:31/12/2008

Abstract:

Many high performance aircraft suffer from a dynamic instability problem at relatively high Mach number and altitude regimes known as Dutch roll instability. In this study the aircraft Dutch-roll and lateral –directional state variables may be enhanced using the yaw damper and washout filter. The Aircraft Dutch-roll damping is improved by identifying a suitable feedback gain matrix plus preserving the airframe's low-frequency behavior by the use of a washout filter with a time constant. An intermediate change in terminology is used to illustrate the procedure for including a washout filter into the aircraft lateral state equation formulation. A stability augmentation system (SAS) and a numerical model constructed for a Mig-21 aircraft are solved to illustrate the proposed procedure. The numerical results show that it was sufficient to use (SAS) including both yaw damper and washout filter to improve the aircraft sideslip angle, roll rate and roll angle response in a short time. Finally, the verification of the aerodynamic characteristics of present model was made by comparing the results of the method used (Low order three dimensional Panel method) with that of Cy-20 aircraft flight data test.

**Keywords:** Dutch roll damping, Yaw damper, Washout filter, Stability augmentation system

## تحليل التدحرج الهولندي ومتغيرات الحالة للطائرة باستخدام مخمد الرحو ومجترف التنقية

الخلاصة

تعاني الكثير من الطائرات ذات الأداء العالي من مشاكل اللاستقرارية الديناميكية عند عدد ماخ وارتفاع عاليين نسبيا بما يدعى التدحرج الهولندي اللااستقراري. في هذه الدراسة تم تحسين التدحرج الهولندي ومتغيرات الحالة الاتجاهية باستخدام مخمد الرحو ومجترف التنقية. لقد تم تحسين إخماد التدحرج الهولندي للطائرة بأستخدام مصفوفة مناسبة للربح بتغذية مرتدة مناسبة بالإضافة إلى المحافظة على تصرف التردد المنخفض للطائرة باستخدام مجترف التنقية بثابت الزمن.

لغرض بيان استخدام مخمد الرحو ومجترف التنقية تم استخدام تغير وسطي جديد باشتقاق معادلات الحركة للطائرة يشمل مخمد الرحو و مجترف التنقية وحل هذه العلاقات . لغرض استعراض هذا الأسلوب المقترح تم تطبيقه على منظومة تعزيز الاستقرارية ونموذجها العددي لطائرة ميك 21 . بينت النتائج العددية كفاءة منظومة تعزيز الاستقرارية بعد إضافة مخمد الرحو ومجترف التنقية اذ تم تحسين زاوية الانحراف الجانبية واستجابة معدل التدحرج وزاوية التدحرج في وقت قصير .

وأخيرا ، لزيادة الوثوقية في حسابات الخصائص الايروديناميكية للموديل الحالي تمت مقارنة الطريقة المستخدمة (طريقة الألواح ثلاثية الأبعاد)مع معلومات فحص الطائرةCy-20 لفحوصات الطيران.

* Mechanical Engineering Department, University of Technology/Baghdad



https://doi.org/10.30684/etj.27.7.11
2412-0758/University of Technology-Iraq, Baghdad, Iraq

# List of symbols

**[A]** Plant matrix

$[B]$ Control sensitivity matrix

$B_R$ Rudder effectiveness control

$CL$ Lift coefficient

$CL_\alpha$ Lift curve slope

$Cm_\alpha$ Pitching moment curve slope

$Cn_r$ Yawing damping derivative

$Cn_\beta$ Directional stability derivative

$G_{\phi\delta}(\omega)$ Gain in roll angle per unit amplitude of rudder deflection (Bode plot)

$G_{p\delta}(\omega)$ Gain in roll rate per unit amplitude of rudder deflection (Bode plot)

$G_{r\delta}(\omega)$ Gain of yaw rate per unit amplitude of rudder deflection (Bode plot)

$G_{\beta\delta}(\omega)$ Gain in sideslip angle per unit amplitude of rudder deflection (Bode plot)

$H$ Height

$I_x$ Moment of inertia in roll

$I_{xz}$ Product of inertia about ox and oz

$[K]$ Feedback matrix

$K_R$ Yaw rate feedback

$L_\beta$ The dihedral effect

$L_p$ The roll damping

$L_r$ The change in rolling moment caused by yawing

$L_\delta$ The change in rolling moment caused by control term

$N_p$ The change in yawing moment caused by rolling

Yaw damping

$N_p$ The change in yawing moment caused by control term

$N_d$ Directional stability

$N_b$ Roll rate

$p$ Yaw rate

$r$ Time constant

$T$ Laplace transformation notation of washout input

$U(s)$ Free stream velocity

$V$ Laplace transformation notation of washout output

$Y(s)$ The change in side force resulting from rolling velocity, change in yawing velocity and change in control term respectively.

$Y_p, Y_r, Y_d$ Phase change in roll rate per unit amplitude of rudder deflection

$\Delta f_{pd}(w)$ Phase change in roll angle per unit amplitude of rudder deflection

$\Delta f_{fd}(w)$ Phase change in yaw rate per unit amplitude of rudder deflection

$\Delta f_{rd}(w)$ Phase change in sideslip angle per unit amplitude of rudder deflection

$\Delta f_{bd}(w)$ Side slip angle

$b$ Roll Angle

$f$ Initial pitch angle

$q_o$ Aileron and rudder deflection

$d_a, d_r$

## 1. Introduction

With the requirements on aircraft to operate at high Mach number and they typically operate at high altitude regimes, the associated flight dynamic have been the subject of much interest recently. The design of jet aircraft with acceptable Dutch roll damping characteristics is a difficult task [1, 2].Both of these factors (Mach and altitude) tend to reduce the damping of Dutch roll mode. For these reason, most jet aircraft are equipped with full-time yaw dampers. Michael [2] suggested a way to improve the Dutch roll damping of jet aircraft by using rudder trailing edge (T-strips) with yaw damper switched off. Research has focused (either experimentally or numerically) on the development of simulation tools for aircraft Dutch roll response to analyze the physics of this mode.

Bruce and Gangsaas [3] presented a method to improve the Dutch roll damping for aircraft operation with autopilot-on and yaw damper-off situation. That was accomplished by computing new feedback gains using control design technique. A full-state feedback system was developed which stabilizes Dutch roll mode at cruise flight conditions.

The previous technique have traditionally developed the yaw damper first to control the rudder, and then designed the autopilot to control the ailerons. The yaw damper system provides aircraft stabilization about the yaw axis and it minimize the Dutch roll during flight the aircraft by providing rudder displacement proportional to, and opposing, the yaw rate of aircraft [4]

In present work a stability augmentation system is designed for Mig-21 aircraft which is modified the Dutch roll damping using the yaw damper and washout filter. The use of a yaw damper as initially described will introduce potential difficulties at low frequency values inasmuch as pilot application of rudder and/or aileron control to initiate a turn command would be countermanded by the negative yaw rate feedback of the yaw damper. The supplementary use of washout filter in the feedback loop is to correct for this influence..

The object of this paper is to enhance the state variables and Dutch roll damping for high performance aircraft in order to illustrate the effect of yaw damper and washout filter on aircraft response.

## 2. Aerodynamic model and stability derivatives of aircraft model

The baseline Mig-21 aircraft is considered in this analysis. The aerodynamic model of the aircraft is a hybrid from model originally used in flight data test Ref. [9] and in work of SED (System Engineering Division) Ref. [10]. According to reference [12] , a modified technique consisting of three dimensional low order panel method supported by semi-empirical skin friction drag model has been used to predict the aerodynamic of a complete Mig-21 fighter aircraft. Semi-empirical formulas of Datcom method have been interacted with the panel results to predict the longitudinal and lateral stability derivatives. Fig.1A,B shows the three dimensional paneling model views of the complete fighter aircraft configuration

Fig.2 [A-E] shows some results of aerodynamic and stability derivatives which are used in the paper.

Also the values of dimensional stability derivatives for Mig-21 aircraft model are shown in Table A1 [Appendix A]. The verification test for aerodynamic analysis have been made to confirm the validity of

computer program results with the available flight data of subsonic and supersonic for aircraft model (Cy-20) [TableA2,Appendix A ] [11]. A good agreement was obtained despite there was about 5-7 % error in lift computations (due to the effects of turbulent flow in transition zone) and supersonic.

## 3. Aircraft lateral-directional equations of motion

The basis for analysis, computation, or simulation of aircraft motions is the mathematical model and its subsidiary systems, i.e their general equations of motion. The aircraft lateral-directional equations of motion in general form can be written as [5]

$$\dot{\beta} = Y_b b + Y_p p + g\cos q_o f + (Y_r - V) r + Y_d d \quad \text{.....(1)}$$

$$\dot{p} - (I_{xz}/I_x)\dot{r} = L_b b + L_p p + L_r r + L_d d \quad \text{.....(2)}$$

$$-(I_{xz}/I_z)\dot{p} + \dot{r} = N_b b + N_p p + N_r r + N_d d \quad \text{.....(3)}$$

$$\dot{f} = p \quad \text{.....(4)}$$

For the purpose of the subsequent analyses, consider the lateral-directional state vector as

$$\{x\} = [b \quad p \quad f \quad r]^T \quad \text{..... (5)}$$

If only rudder or aileron control were under consideration, then the control input would simplify to a single (scalar) value. The plant matrix is expressed as

$$[A] = \begin{bmatrix} Y_b/V & Y_p/V & g\cos q_o/V & (Y_r - V)/V \\ L_b & L_p & 0 & L_r \\ 0 & 1 & 0 & 0 \\ N_b & N_p & 0 & N_r \end{bmatrix} \quad \text{.....(6)}$$

whereas the control sensitivity matrix is

$$[B] = \begin{bmatrix} Y_{dr}/V & Y_{da}/V \\ L_{dr} & L_{da} \\ N_{dr} & N_{da} \end{bmatrix} \quad \text{....(7)}$$

## 4. Yaw damper design for stability augmentation

The yaw damper for the purpose of improving aircraft Dutch-roll model damping will be designed using state variable feedback concept. A yaw damper may be viewed as a form of stability augmentation with its goal the improvement of aircraft handling qualities. An elementary form of the state vector block diagram with the addition of negative state vector feedback via a gain matrix is shown in Fig.3. The command information to the rudder is assumed as coming from either pilot input or state vector feedback. The solid lines in Fig.3 represent scalar terms whereas the dash lines represent vector quantities.

The elements shown in Fig.3 are defined as follow:

$\{x\}$ is state vector, $[A]$ is unaugmented plant matrix, $B_R$ is rudder effectiveness control and $d_{rF}$ is feedback input command to rudder control.

The feedback matrix will initially be assumed as consisting only of a yaw rate entry $K_r$. Therefore, $[K]$ will have the form

$$[K] = [0 \quad 0 \quad 0 \quad K_r]$$

The dual rudder inputs alter the state

equation slightly to

$$\{\dot{x}\} = [A]\{x\} + \{B_R\}(d_{rP} + d_{rF}) \quad \ldots(8)$$

Where the rudder deflection due to the yaw damper feedback is defined as:

$$d_{rF} = -[K]\{x\} \quad \ldots(9)$$

Combining the rudder feedback term into the state equation provides an augmented plant matrix in the form of

$$\{\dot{x}\} = [A - B_R K]\{x\} + \{B_R\}d_{rP} \quad \ldots.(10)$$

where the augmented matrix is $[A - B_R K]$.

5. Application of a Washout filter

There is a potential for a conflict with simplified yaw damper model described in previous section. Pilot inputs will normally occur in frequency range considerably lower than Dutch-roll modal frequency; however, the yaw damper considered up to this point will provide rate-dependent feedback to the rudder regardless of the frequency; however, the yaw damper considered up to this point will provide rate-dependent feedback to rudder regardless of the frequency. A pilot command to the rudder or a turn will incur an augmentation command to suppress the airframe's yaw rate. A suitable approach to avoid the potential difficulty of using single control surface for multiple purposes is to include an appropriate filter in the feedback circuit. For the case of a yaw damper, the influence of state vector feedback can be effectively removed at low frequencies by introducing a washout filter in the feedback circuit. The washout filter resembles a low-pass filter in the denominator while containing an $s$ in the numerator to decrease the gain below the corner frequency ,While the washout filters facilitate automatic following of a targeted operating point, which results in vanishing control energy once stabilization is achieved and steady state is reached.Although there is no systematic way for choosing the constants of the washout filters and the control parameters [6-8].

with the corresponding frequency response being

$$G(iw) = \frac{iw}{1+iwT} = \frac{w}{\left[1+(wT)^2\right]^{1/2}} e^{i(f+p/2)}$$

…….(11)

where $f = \tan^{-1}(-wT)$

Blocks diagrams showing the principle of a washout filter from two different viewpoints are shown in Fig.4

Figure 4a shows in Laplace transform notation the relation between input $Y(s)$ and output

Which factors to

$$Y(s) = \frac{s}{(1+Ts)} U(s) = G(s)U(s)$$

……(12)

In the time domain, equation (12) readily translates to

$$(\dot{y}) + (1/T)y = (1/T)(\dot{u})$$

…….(13)

The problem with equation (13) is that it is not in a convenient state vector arrangement due to the derivative action on the input. A way to circumvent this difficulty is to define $y$ in terms of $u$ and new state variable $x_5$, i.e.

$$y = (1/T)u - (1/T)x_5 \quad \ldots\ldots(14)$$

along with

$$\dot{x}_5 = -(1/T)\,x_5 + (1/T)\,u \qquad (15)$$

It is straightforward to show that equation (14) and (15) satisfy equation (13). The added state variable $x_5$, which in general will not have a physical meaning, is a technique used to preserve a state variable solution procedure in the presence of inputs with the time derivatives. Fig. 4b is the state variable format of the washout filter and is consistent with equations (18) and (19). The use of a washout filter in the feedback circuit of the yaw damper is shown in Fig.5. In this figure $d_{rP}$ used as the input of the system, also it is possible to use the aileron and rudder as the input [13]. The state variable format for the washout filter has been sketched into the feedback loop between the output of the gain matrix $[K]$ and the negative feedback summation of $d_{rF}$.

$$y = (1/T)[K]\{x\} - (1/T)\,x_5 \qquad ..(16)$$

then

$$\{\dot{x}\} = [A]\{x\} + [B_R]d_{rF} + \{B_R\}d_{rP}$$

Alter the state equation relations to

$$\dot{x} = [A - (1/T)B_R K]\{x\} + (1/T)\{B_R\}x_5 + \{B_R\}d_{rP} \qquad ……..(17)$$

plus the added term to account for $x_5$

$$\dot{x}_5 = (1/T)[K]\{x\} - (1/T)\,x_5 \qquad …(18)$$

The presence of washout filter has increased the size of the state vector from (4x1) to (5x1) due to the addition of $x_5$ term. The state equation can be viewed in its partitioned form as equivalent to equation (18).This approach preserve the matrix algebra tools used up to now to solve the eigenvector problem. Here,

$$\begin{Bmatrix} \{\dot{x}\} \\ \dot{x}_5 \end{Bmatrix} = \begin{bmatrix} A - (1/T)B_R K & (1/T)B_R \\ (1/T)K & -(1/T) \end{bmatrix} \begin{Bmatrix} \{x\} \\ x_5 \end{Bmatrix} + \begin{Bmatrix} B_R \\ 0 \end{Bmatrix} d_{rP} \qquad ……(19)$$

Equation (19) makes possible a lateral-directional analysis using software tools for the purpose of improving Dutch-roll damping by identifying suitable feedback matrix $[K]$ plus preserving the airframe's low-frequency behavior by the use of a washout filter with a time constant.

**6. Results and Discussion**

Mig-21 aircraft with Mach number $M = 0.6$ and height $H = 10Km$, was taken into consideration in this analysis in order to demonstrate the state variables behavior and response of aircraft including yaw damper and washout filter to enhance the mentioned variables. The results indicated that the transfer function of the original model (without yaw damper and wash out filter) is

The lateral-directional equations of motion as function of state variables time response was solved in present work for the original model. A time history plot of $b$, $p$ and $f$ due to the assumed rudder control impulse for a time span of time=0-15 sec is shown in Fig.6.The exponential decay of the sideslip angle response in Fig.6 to an impulse like rudder input shows the properties of a lightly damped Dutch-roll mode. However, the rudder impulse input excited all of the modes including the roll and spiral modes.

A Bode plot showing the harmonic response of the lateral-directional state vector components per unit amplitude of

the rudder deflection is shown in Fig.7A. Agreement with this approximation is found by noting that $G_{bd}(w)$ has a constant value until the neighborhood of the modal frequency.Byoned the modal frequency, the gain changed at -40 dB per decade. The phase angle curve also shows a -180 deg change when comparison is made at frequencies before and after the modal frequency as shown in Fig.7B.A Bode plot that reflects the harmonic response behavior due to aileron deflection is shown in Fig.8A, B.

The unaugmented value of damping ratio for original model is 0.0777 according to the equation $[V = 0.5(-N_r)/\sqrt{N_b}]$. To find the value of rate feedback $K_r$ ,in the gain matrix of $[K]$ in order to increase the Dutch-roll modal damping to $V = 0.2, 0.3$ and to maximum value 0.45 (tested value), The augmented matrix can be established a feedback row vector $[K]$ has been assumed followed by verification that the desired damping ratio has been obtained.

In finding the appropriate feedback constant, iteration was done until the desired damping level was determined. The numerical results indicated that the value of $K_r = -0.506, -0.880$ and -1.5 s for $V = 0.2, 0.3$ and 0.45. These behaviors can be shown from the yaw damper root locus in Figures 9 and 10. The effect of yaw damper influence comparison with the original model in both gain and phase can be displayed in Bode plot of Fig.11.

A new plant matrix and the new control surface matrix of yaw damper

(Original model+ yaw damper)

and washout filter are adding

An improvement in sideslip angle, roll rate and roll angle are achieved according to existence of yaw damper. The influence can be noted in Figures 12 , 13 and 14.

9 A washout filter was added to the yaw damper feedback circuit. The Bode plot (Fig.15) shows the influence of the washout filter in achieving the stated goal. It can be seen in Fig.15a, that the reduction in Dutch-roll damping from $V = 0.3$ to $V = 1.65$ due to the presence of the washout filter is evident as an increase in decibels of the gain $G_{rdr}$ in the neighborhood of the Dutch-roll frequency. However, in the low-frequency range, corresponding to aircraft operations in steady turns and/or slow pilot control inputs, both the $G_{rdr}$ gain and the phase angle functions for the yaw damper plus washout filter are nearly identical to those for the basic airframe. The effect of the washout filter on modal damping is achieved by applying equation 19.

$$\frac{-0.72s^4 - 0.13s^3 + 0.032s^2 + 0.023s + 0.007}{s^5 + 1.04s^4 + 1.48s^3 + 0.919s^2 + 0.14s - 0.0027}$$

preserving the airframe's low-frequency behavior of a washout filter with a time constant is used. The influence of the

8 Dutch roll damping for the original model (without yaw damper and washout filter) was found to be weak. Furthermore the following conclusions have been obtained in present paper:

## 7. Conclusions

The enhancement of the Dutch-roll mode damping and state variables of high performance aircraft is analyzed including the yaw damper and washout filter. A suitable feedback matrix $[K]$ plus

1- An intermediate change in terminology or methodology have been used to illustrate the procedure for including a washout filter into the original state equation formulation
2- The time response of state variables including the sideslip angle ,roll rate and roll angle has been enhanced according to(Fig.12,13 and 14)
3- The result indicated that the $N_r$ stability derivative has the dominant influence on a yaw damper effect and on the root migration.

**References**

[1] Emad N Abdulwahab, Chen Hongquan, "Periodic motion suppression based on control of wing rock in aircraft lateral dynamics", Aerospace Science and Technology,Vol.12,pp:295-301, 2008

[2] Michael A.Cavanauugh, "The use of rudder trailing edge T-strips to improve Dutch roll damping", AIAA Atmospheric Flight Mechanics Conference and Exhibit, 11-14 August, 2003, Austin, Texas

[3] K.R.Bruce and D.Gangsaas, "Improvement of the 767 lateral autopilot using optimal control design technique", AIAA paper 43485, 1984

[4] Isaac K.,Russell A.,Edward E and Yaghoob S., "Design of integrated pitch axis for autopilot / autothrottle and integrated lateral axis for autopilot/yaw damper for NASA TSRV airplane using integral LQG methodology", NASA contractor report 4268,1990.

[5] L. V. Schmidt, "Introduction to aircraft flight dynamics", Naval Postgraduate School, AIAA Education Series, Monterey, California, 1998.

[6] H. C. Lee and E. H. Abed, "Washout filters in the bifurcation control of high alpha flight dynamics," in Proceedings of the American Control Conference, Boston, MA, 1991, pp. 206–211.

[7] E. H. Abed, H. O. Wang, and R. C. Chen, "Stabilization of period doubling bifurcations and implications for control of chaos," *Physica D*, vol. 70, no. 1-2, pp. 154–164, Jan 1994.

[8] H. O. Wang and E. H. Abed, "Bifurcation control of a chaotic system," *Automatica*, vol. 31, no. 9, pp. 1213–1226, Sep 1995.

[9] Aircraft MIG-21 BIS/Fished-N, Aerodynamic Characteristics, Technical Description Manual.1975.

[10]S.Balakrishna, and et al. (SED), "Stability and control characteristics of fighter aircraft", Special publication ,India,1989

[11] Aircraft Cy-20, Technical Description, Book 1. General information and flight performance . No. 28, 1972.

[12] Emad, N.Abdulwahab" Numerical investigation of roll inertia cross coupling and its effects on stability and response of supersonic aircraft", Ph.D.Thesis, Dept. of Aeronautics Engineering, University of Technology, Baghdad, 2003

[13] John H.Blackelock"Automatic control of aircraft and missile", John Wiley & Sons.Inc,1965

# Appendix A

Table A1: Stability derivatives Mig-21aircraft with Mach =0.6: H=10Km.

| $y_b$ | $L_b$ | $L_p$ | $L_r$ | $N_b$ | $N_p$ | $N_r$ | $Y_d$ | $L_d$ | $N_d$ |
|---|---|---|---|---|---|---|---|---|---|
| **m/sec$^2$** | **1/sec$^2$** | **1/sec** | **1/sec** | **1/sec$^2$** | **1/sec** | **1/sec** | **m/sec$^2$** | **1/sec$^2$** | **1/sec$^2$** |
| **-4.62** | **-11.15** | **-0.479** | **0.248** | **1.34** | **0.069** | **-0.016** | **0.022** | **6.3446** | **-0.7233** |

**Table A2: Aerodynamic Characteristics Comparison Results**

| | **Mach No.** | **Flight Data [11]** | **Present Work** | **Error %** |
|---|---|---|---|---|
| $C_{La}$ / deg. | **0.8** | **0.0541** | **0.0505** | **-7.0** |
| | **1.3** | **0.0607** | **0.0575** | **-5.5** |
| $C_{D0}$ | **0.8** | **0.0171** | **0.0162** | **-5.5** |
| | **1.3** | **0.0393** | **0.0382** | **-2.8** |

Appendix B: The three views of Mig-21 aircraft and remote axis selection

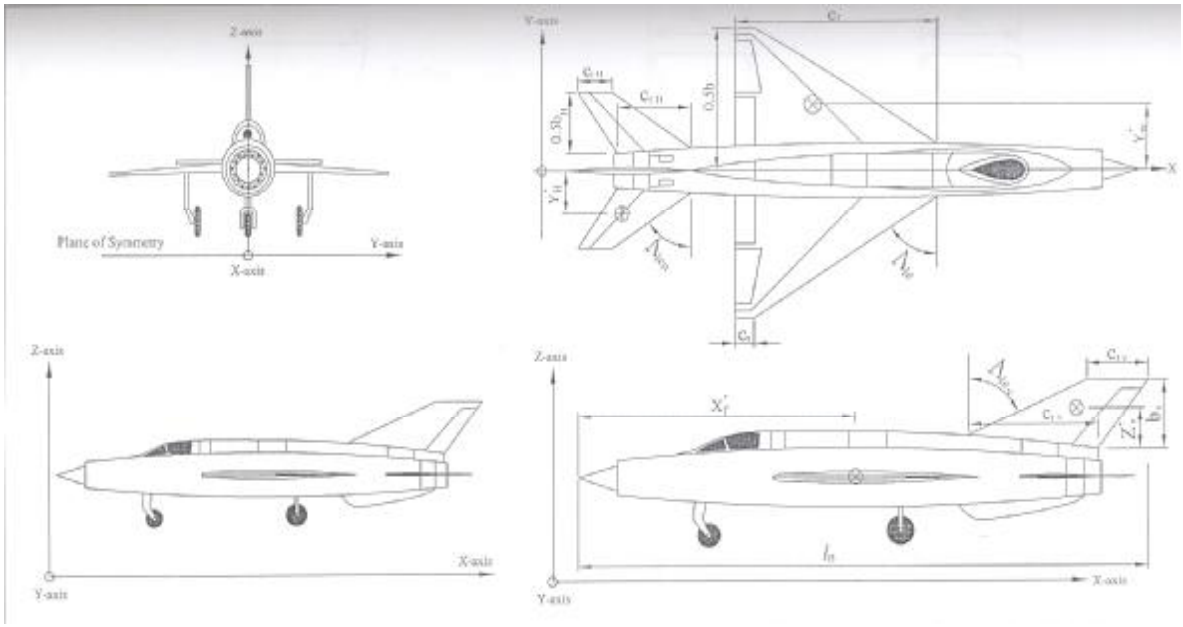

**1. Fuselage :**

| | |
|---|---|
| Total overall length | 12.8 m |
| Maximum depth | 1.26 m |
| Maximum width | 1.07 m |

**2. Wing**

| | |
|---|---|
| Airfoil section | 0006 |
| Area | 23 $m^2$ |
| Span | 7.15 m |
| Swept angle | 57 deg |
| Thickness to chord ratio | 0.044 |
| Area of control surface (flap + aileron) | 1.117 $m^2$ |
| Exposed root chord | 6.0 m |
| Tip chord | 0.45 m |
| Mean aerodynamic chord | 4.0 m |
| Aspect ratio | 2.22 |

**3. Horizontal tail**

| | |
|---|---|
| Exposed area | 3.78 $m^2$ |
| Span | 3.6 m |
| Root chord | 1.9 m |
| Tip chord | 0.9 m |
| Swept angle | 55 deg |

**4.Vertical tail**

| | |
|---|---|
| Exposed area | 5.27 $m^2$ |
| Span | 2.0 m |
| Tip chord | 1.47 m |
| Root chord | 3.8 m |

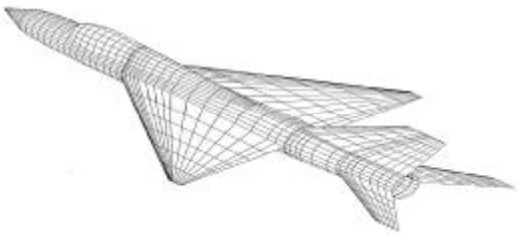

[A]

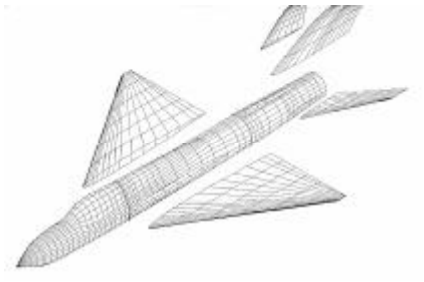

[B]

**Fig.1 A,B Three dimensional paneling model views of the complete fighter Mig-21aircraft configuration**

[A]

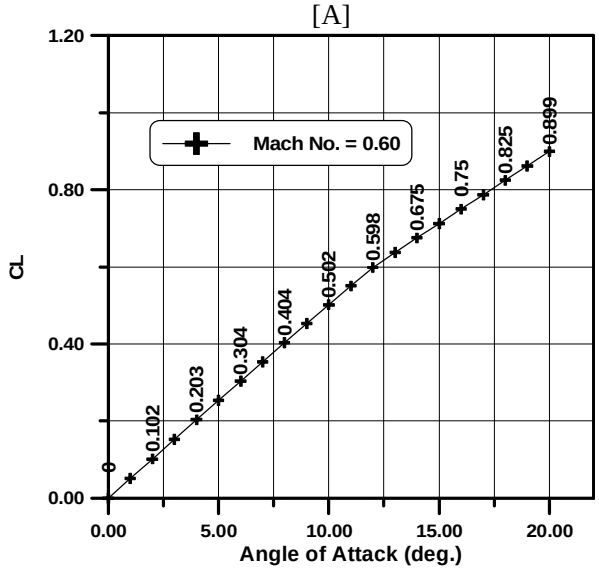


[B]

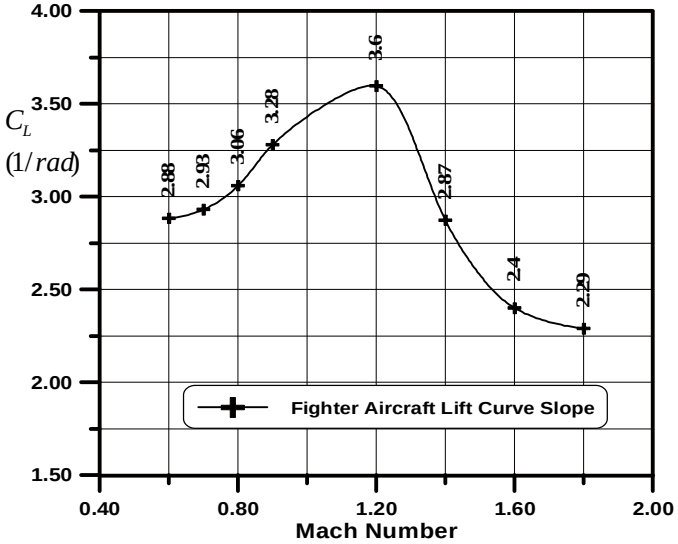


[C]

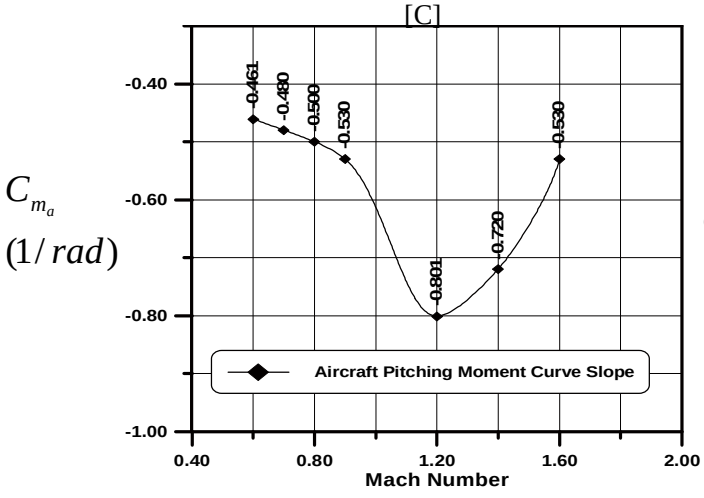


[D]

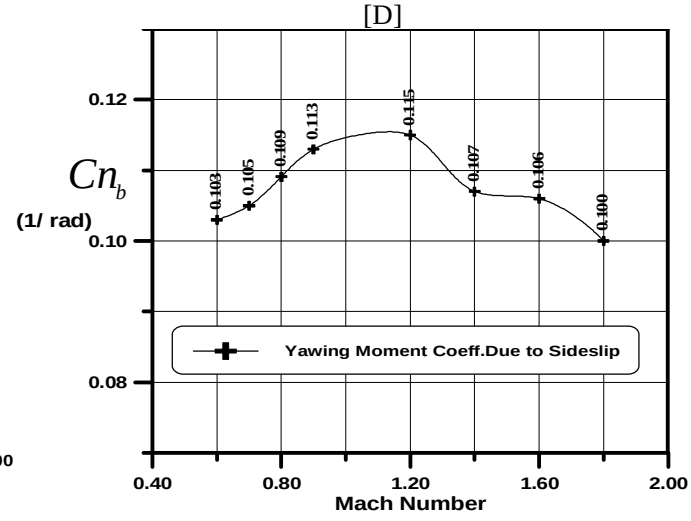

[E]

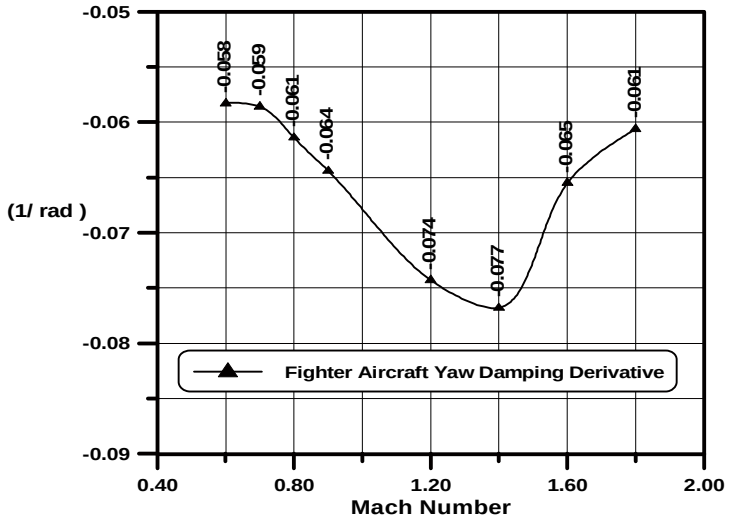


**Fig.2 [A] Mig-21 lift coefficient vs angle of attack**
**[B] Aircraft lift curve slope**
**[C] Aircraft pitching moment curve slope**
**[D] Aircraft directional stability derivative**

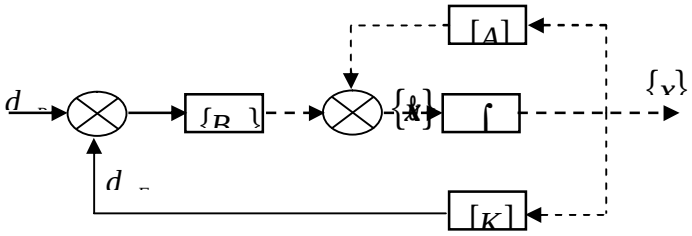


**Fig.3 Block diagram of a closed-loop**

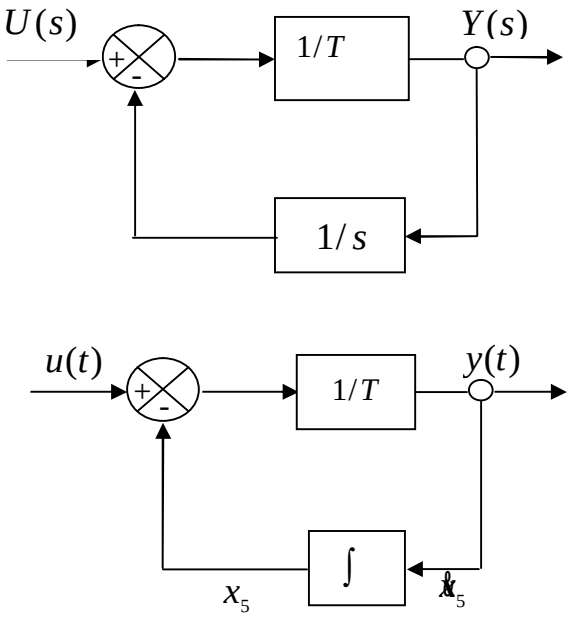


**Fig.4 Washout filter block diagrams**

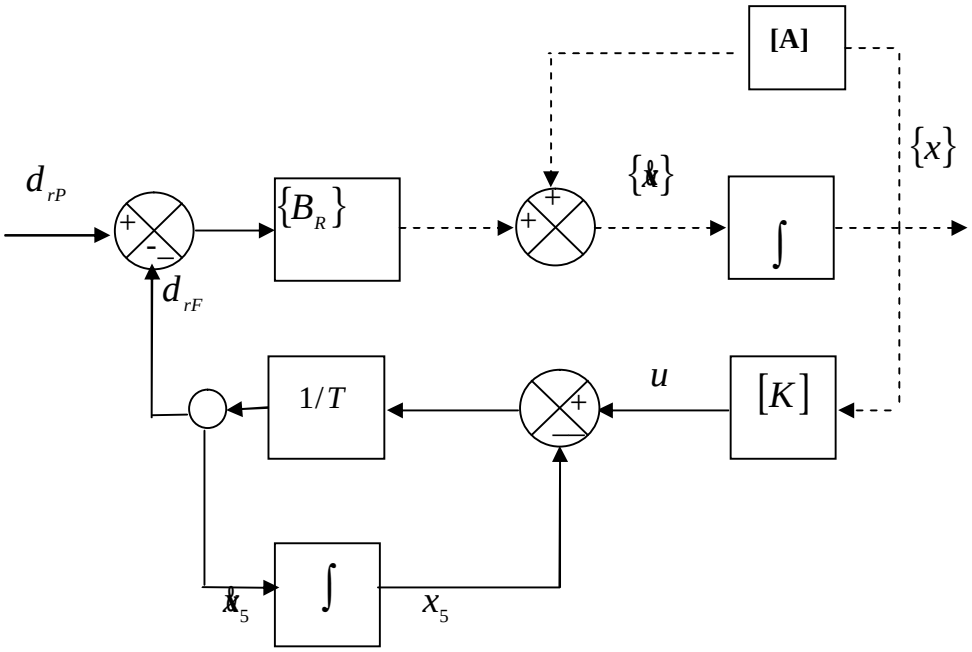


**Fig.5 Block diagram, yaw damper plus washout filter filter**

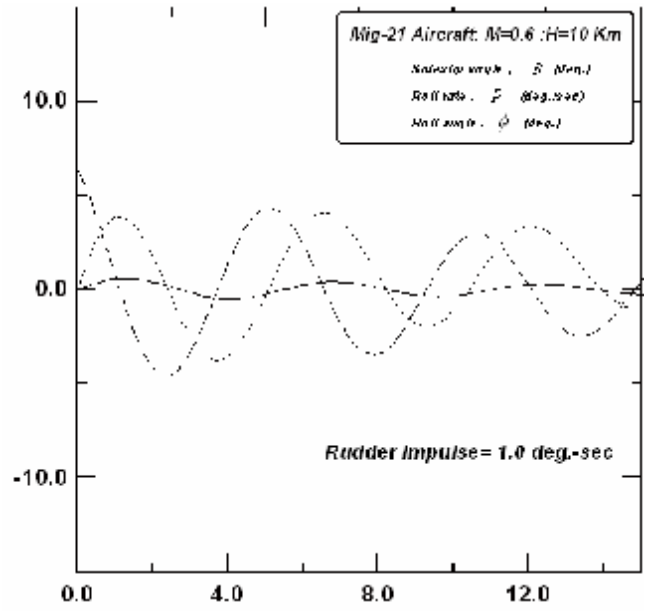


**Fig.6 Original aircraft response due to a rudder**

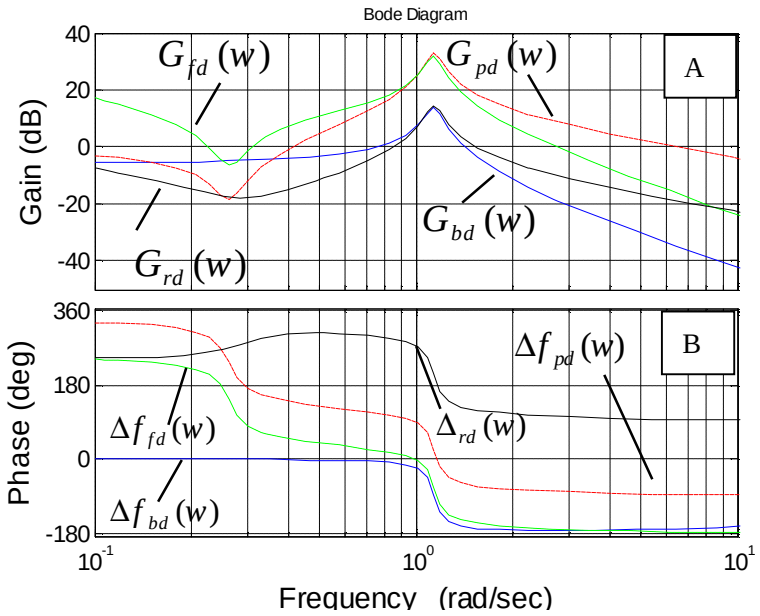


**Fig.7 Frequency response, harmonic rudder input**
**for Mig-21 aircraft.**
**[A] Gain vs. frequency**

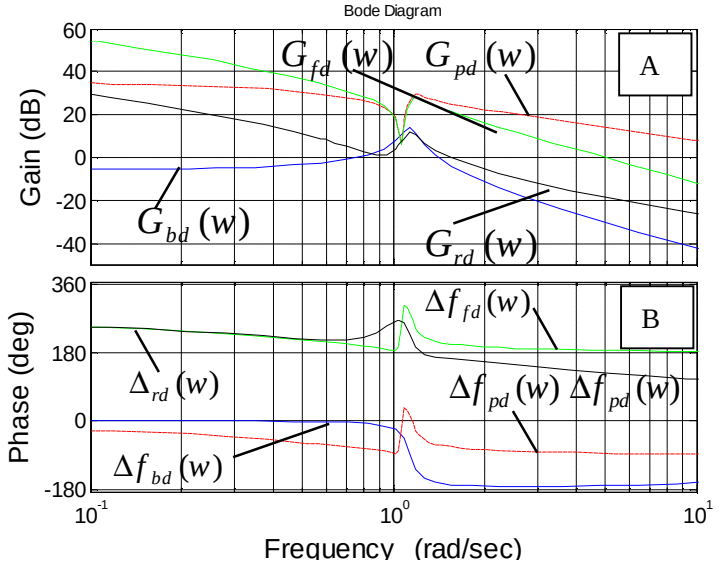


**Fig.8 Frequency response, harmonic aileron input**
**for Mig-21 aircraft.**
**[A] Gain vs. frequency**
**[B] Phase vs. frequency**

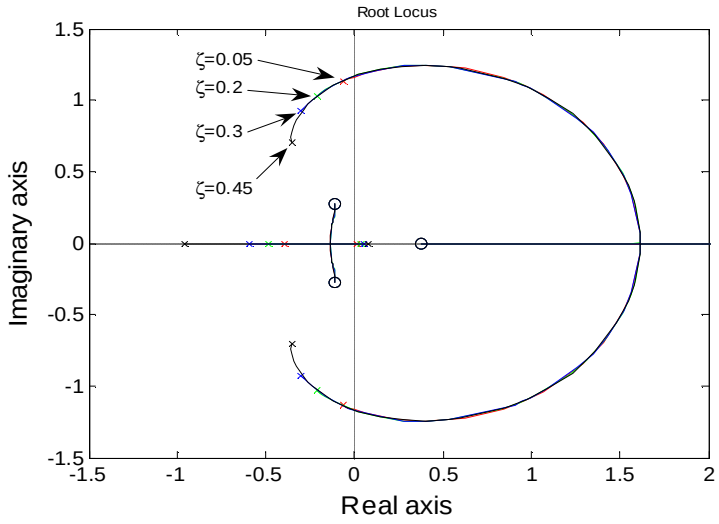


**Fig.9 Yaw damper root locus**

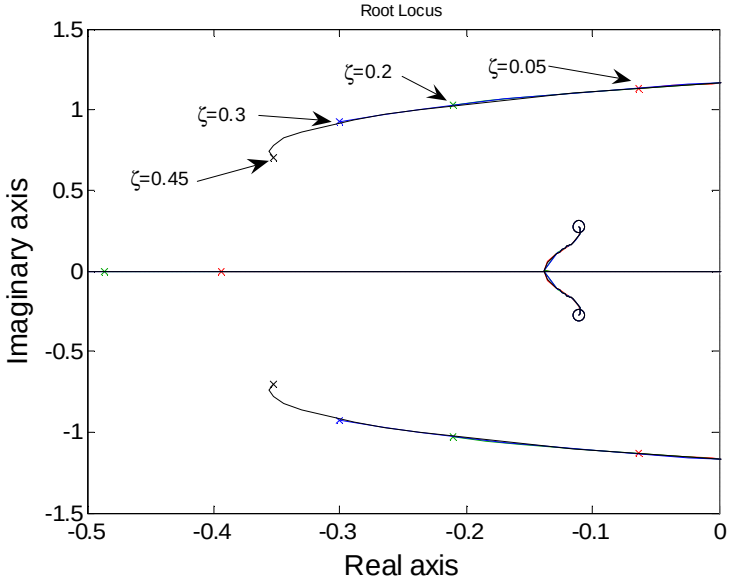


**Fig.10 More details of yaw damper root locus**

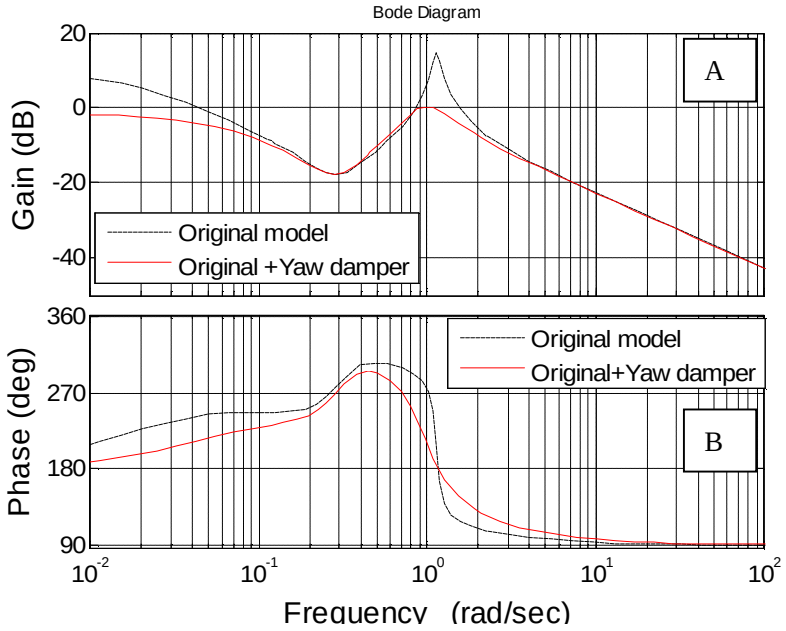


**Fig.11 Bode plot showing yaw damper influence**

**for Mig-21 aircraft.**

**[A]** $G_{rd\,r}$ **vs. frequency**

**[B]** $\Delta f$ **vs. frequency**

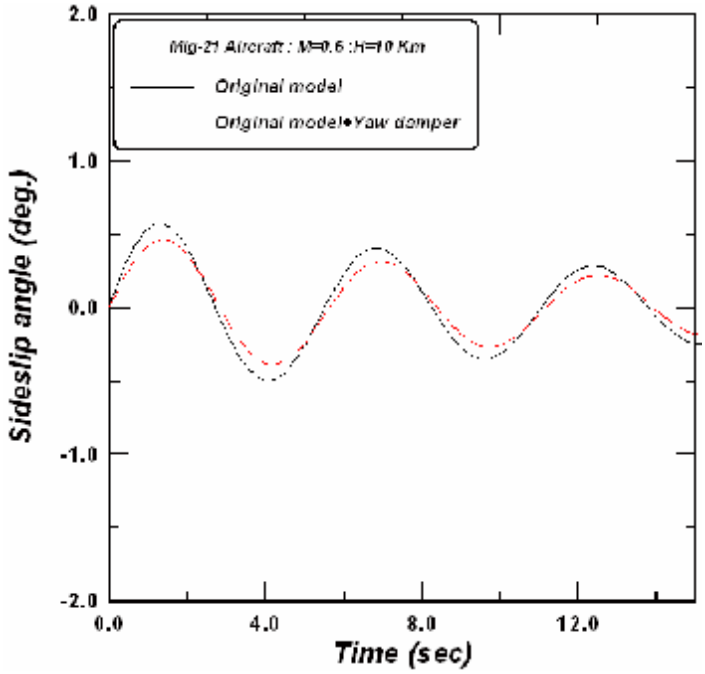


**Fig.12 Effect of yaw damper on sideslip angle**

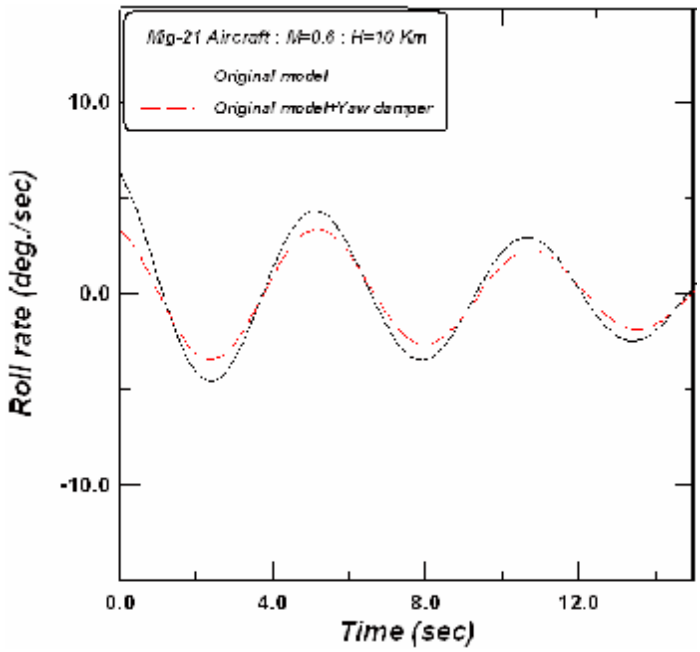


**Fig.13 Effect of yaw damper on roll rate**

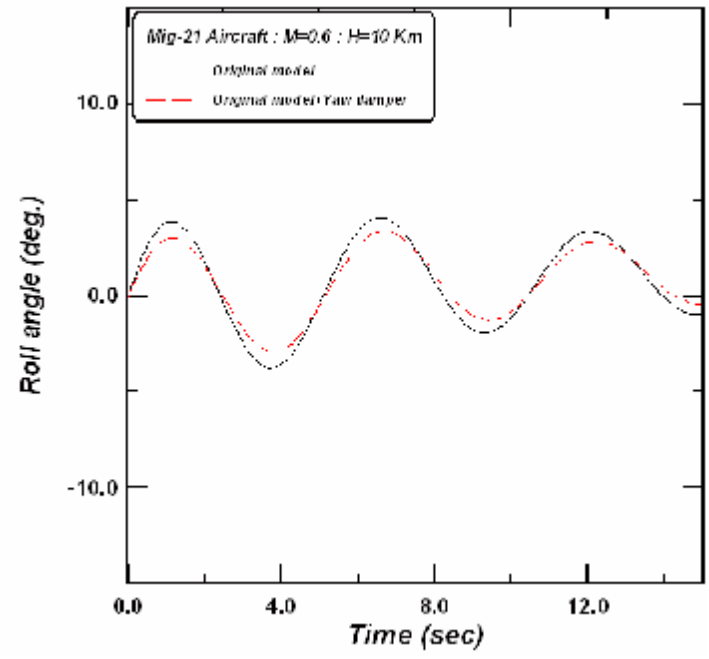


**Fig.14 Effect of yaw damper on roll angle**

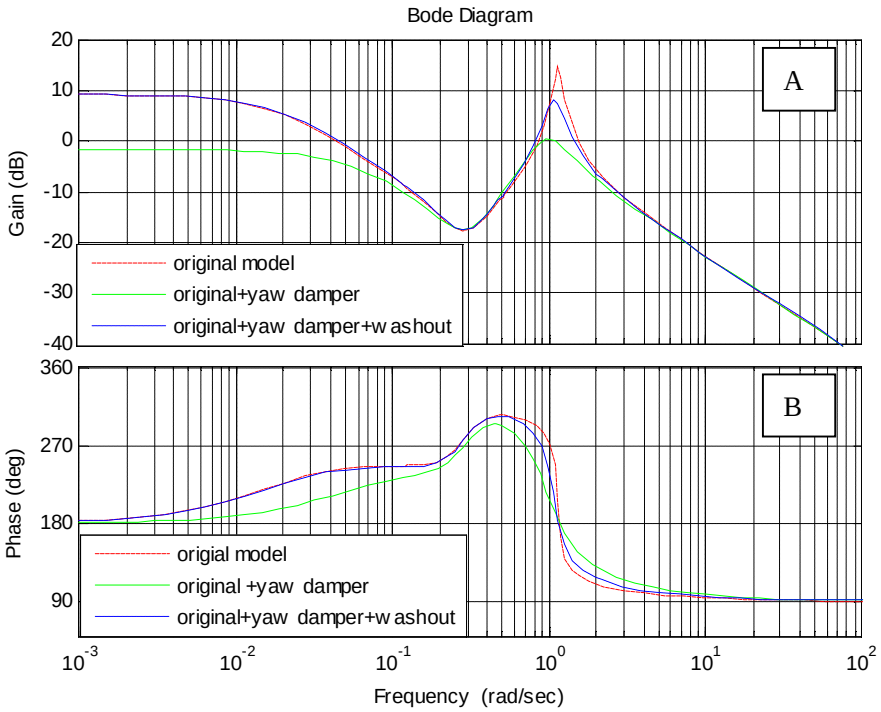


**Fig.15 Bode plot showing washout influence for Mig-21 aircraft.**

**[A]** $G_{rd\,r}$ **vs. frequency** **[B]** $\Delta f_{rd\,r}$ **vs. frequency**